The University of Sydney
School of Mathematics and Statistics

Assignment 2

MATH1002: Linear Algebra — Semester 1, 2022

Lecturers: Bregje Pauwels, Anne Thomas

This **individual** assignment is due by **11:59pm Monday 9 May 2022**, via Canvas. Late assignments will receive a penalty of 5% per day until the closing date. A single PDF copy of your answers must be uploaded in Canvas at https://canvas.sydney.edu.au/courses/40182. It should include your SID. Please make sure you review your submission carefully. What you see is exactly how the marker will see your assignment. Submissions can be overwritten until the due date. To ensure compliance with our anonymous marking obligations, please do not under any circumstances include your name in any area of your assignment; only your SID should be present. The School of Mathematics and Statistics encourages some collaboration between students when working on problems, but students must write up and submit their own version of the solutions. If you have technical difficulties with your submission, see the University of Sydney Canvas Guide, available from the Help section of Canvas.

This assignment is worth 10% of your final assessment for this course. Your answers should be well written, neat, thoughtful, mathematically concise, and a pleasure to read. Please cite any resources used and show all working. Present your arguments clearly using words of explanation and diagrams where relevant. After all, mathematics is about communicating your ideas. This is a worthwhile skill which takes time and effort to master. The marker will give you feedback and allocate an overall mark to your assignment using the following criteria:

Rubric

Criteria	Ratings							Pts
Correct solutions to the questions	**8 pts** **Excellent** Excellent work, answering all parts correctly. There are at most only minor or trivial errors or omissions.	**7 pts** **Very good work** Making very good progress but with one or two substantial errors, misunderstandings or omissions throughout the assignment.	**6 pts** **Good work** Making good progress, but making more than two distinct substantial errors, misunderstandings or omissions throughout the assignment.	**5 pts** **Fair work** A reasonable attempt, but making more than three distinct substantial errors, misunderstandings or omissions throughout the assignment.	**3 pts** **Poor** Some attempt, with limited progress made.	**1 pts** **Extremely poor** Extremely limited attempt.	**0 pts** **No Marks** No credit awarded.	8 pts
Clear explanations, diagrams and working shown	**2 pts** **Full Marks** Criteria met.	**1 pts** **Partial marks** Some explanations given.	**0 pts** **No Marks** No clear explanations.					2 pts
								Total Points: 10

1. *In this question, you will be using the following trigonometric identities:*

$$\cos^2\alpha + \sin^2\alpha = 1 \tag{1}$$
$$\cos(\alpha+\beta) = \cos\alpha\cos\beta - \sin\alpha\sin\beta \tag{2}$$
$$\sin(\alpha+\beta) = \sin\alpha\cos\beta + \cos\alpha\sin\beta \tag{3}$$

where $\alpha, \beta \in \mathbb{R}$. You do not need to prove these identities. You may also use without proof the fact that the set

$$\left\{ \begin{bmatrix} \cos\alpha \\ \sin\alpha \end{bmatrix} : \alpha \in \mathbb{R} \right\}$$

is exactly the set of unit vectors in $\mathbb{R}^2$.

Now for any real number α, define

$$R_\alpha = \begin{bmatrix} \cos\alpha & -\sin\alpha \\ \sin\alpha & \cos\alpha \end{bmatrix}$$

(a) Prove that for all $\alpha, \beta \in \mathbb{R}$,

$$R_\alpha R_\beta = R_{\alpha+\beta}$$

(b) Using part (a), or otherwise, prove that R_α is invertible and that $R_\alpha^{-1} = R_{-\alpha}$, for all $\alpha \in \mathbb{R}$.

(c) Prove that for all $\alpha \in \mathbb{R}$ and all $\mathbf{x}, \mathbf{y} \in \mathbb{R}^2$,

$$(R_\alpha \mathbf{x}) \cdot (R_\alpha \mathbf{y}) = \mathbf{x} \cdot \mathbf{y}$$

(d) Suppose A is a 2×2 matrix such that for all $\mathbf{x}, \mathbf{y} \in \mathbb{R}^2$,

$$(A\mathbf{x}) \cdot (A\mathbf{y}) = \mathbf{x} \cdot \mathbf{y}$$

Must it be true that $A = R_\alpha$, for some $\alpha \in \mathbb{R}$? Either prove this, or give a counterexample (including justification).

(e) Let $B = \begin{bmatrix} a & b \\ c & d \end{bmatrix}$ be any 2×2 matrix.

(i) Show that there are real numbers u_{11} and α such that $\begin{bmatrix} a \\ c \end{bmatrix} = u_{11} \begin{bmatrix} \cos\alpha \\ \sin\alpha \end{bmatrix}$.

(ii) Let $\alpha \in \mathbb{R}$. Use the invertibility of R_α to prove that there are unique $u_{12}, u_{22} \in \mathbb{R}$ such that

$$\begin{bmatrix} b \\ d \end{bmatrix} = u_{12} \begin{bmatrix} \cos\alpha \\ \sin\alpha \end{bmatrix} + u_{22} \begin{bmatrix} -\sin\alpha \\ \cos\alpha \end{bmatrix}$$

(iii) Use parts (i) and (ii) to show that B can be expressed in the form

$$B = R_\alpha U$$

for some $\alpha \in \mathbb{R}$ and some upper-triangular matrix U.

(iv) Suppose that $B = R_\alpha U = R_\beta V$, where $\alpha, \beta \in \mathbb{R}$ and U and V are upper-triangular. Prove that if B is invertible, then $U = \pm V$.

2. *Some parts of this question refer to the attached research paper:*

Mili Shah (2013), Solving the Robot-World/Hand-Eye Calibration Problem Using the Kronecker Product, Journal of Mechanisms and Robotics, Volume 5, Issue 3 (2013).

(a) A *rotation matrix* is a 3×3 matrix R such that $\det(R) = 1$ and $R^{-1} = R^T$. Let R and S be rotation matrices, and let $\mathbf{t}, \mathbf{u} \in \mathbb{R}^3$.

(i) Prove that RS is a rotation matrix.

(ii) Given $R = \begin{bmatrix} r_{11} & r_{12} & r_{13} \\ r_{21} & r_{22} & r_{23} \\ r_{31} & r_{32} & r_{33} \end{bmatrix}$ and $\mathbf{t} = \begin{bmatrix} x \\ y \\ z \end{bmatrix} \in \mathbb{R}^3$, we write $\begin{bmatrix} R & \mathbf{t} \\ 0 & 1 \end{bmatrix}$ for the 4×4 matrix

$$\begin{bmatrix} r_{11} & r_{12} & r_{13} & x \\ r_{21} & r_{22} & r_{23} & y \\ r_{31} & r_{32} & r_{33} & z \\ 0 & 0 & 0 & 1 \end{bmatrix}.$$

From page 1 of the attached paper, the product

$$\begin{bmatrix} R & \mathbf{t} \\ 0 & 1 \end{bmatrix} \begin{bmatrix} S & \mathbf{u} \\ 0 & 1 \end{bmatrix}$$

is a matrix of the form $\begin{bmatrix} R' & \mathbf{v} \\ 0 & 1 \end{bmatrix}$, where R' is a rotation matrix and $\mathbf{v} \in \mathbb{R}^3$. Write down expressions for R' and $\mathbf{v}$ in terms of R, S, $\mathbf{t}$ and $\mathbf{u}$. *For this question only, you do not need to give any reasons for your answer.*

(b) Suppose a robot is posed n times, leading to the equations

$$R_{A_j} R_X = R_Y R_{B_j}$$

where R_{A_j}, R_X, R_Y and R_{B_j} are rotation matrices, for $j = 1, 2, \ldots, n$. Write a few sentences to summarise the results of the attached paper by Shah on:

(i) the number of poses needed to obtain unique matrices R_X and R_Y which satisfy these equations; and

(ii) how the position errors for the method presented in the attached paper compare to the position errors for the method of Li et al, on simulated data and real-world data.

Solving the Robot-World/Hand-Eye Calibration Problem Using the Kronecker Product

Mili Shah
Department of Mathematics and Statistics
at Loyola University Maryland,
4501 North Charles Street,
Baltimore, MD 21210;
Intelligent Systems Division at National Institute
of Standards and Technology (NIST),
100 Bureau Drive,
Gaithersburg, MD 20899
e-mail: mishah@loyola.edu

This paper constructs a separable closed-form solution to the robot-world/hand-eye calibration problem $\mathbf{AX} = \mathbf{YB}$. *Qualifications and properties that determine the uniqueness of* $\mathbf{X}$ *and* $\mathbf{Y}$ *as well as error metrics that measure the accuracy of a given* $\mathbf{X}$ *and* $\mathbf{Y}$ *are given. The formulation of the solution involves the Kronecker product and the singular value decomposition. The method is compared with existing solutions on simulated data and real data. It is shown that the Kronecker method that is presented in this paper is a reliable and accurate method for solving the robot-world/hand-eye calibration problem.*
[DOI: 10.1115/1.4024473]

Keywords: robotics, computer vision, robot-world calibration, hand-eye calibration, six degrees of freedom, translation, rotation, camera calibration, registration

1 Introduction

As computer vision systems advance technologically and become more pervasive, the need for more sophisticated and effective methods to evaluate their accuracy grows. One method to evaluate a given computer vision system is to compare the data it gathers with data from another more reliable system considered ground truth. However, there are problems with directly comparing the two systems' data, since each system gathers data with respect to its own coordinate frame. For instance, consider the experimental setup of Fig. 1. Here there are two systems: a computer vision system and a precise sensor system considered ground truth. Both the camera for the computer vision system and the target for the sensor system are rigidly attached to a moving robot arm with a fixed unknown transformation $\mathbf{Y}$ between them. The target is being tracked at positions $j = 1, 2, \ldots, n$ by a stationary sensor with its data being represented as $\mathbf{A}_j$, while simultaneously the camera is tracking a stationary object at positions $j = 1, 2, \ldots, n$ with its data being represented as $\mathbf{B}_j$. There is a fixed unknown transformation $\mathbf{X}$ between the stationary sensor and object. Looking at this setup, one can easily see that both $\mathbf{A}_j$ and $\mathbf{B}_j$ are calculated with respect to their own coordinate frame. However, if the unknown transformations $\mathbf{X}$ and $\mathbf{Y}$ could be found, then one could transform the coordinate frame of the computer vision system data to the coordinate frame of the ground truth data. Then, one could directly compare the given computer vision system data with the ground truth data. In this paper, we construct closed-form solutions for $\mathbf{X}$ and $\mathbf{Y}$ using the Kronecker product.

The unknowns $\mathbf{X}$ and $\mathbf{Y}$ can be constructed by solving the robot-world/hand-eye calibration problem

$$\mathbf{A}_j\mathbf{X} = \mathbf{Y}\mathbf{B}_j$$

at positions $j = 1, 2, \ldots, n$. Here, $\mathbf{X}$, $\mathbf{Y}$, $\mathbf{A}_j$, and $\mathbf{B}_j$ are represented as homogeneous matrices of the form

$$\begin{pmatrix} \mathbf{R} & \mathbf{t} \\ 0 & 1 \end{pmatrix}$$

where orientation is represented as the 3×3 rotation matrix $\mathbf{R}$ and position is represented as the 3×1 vector $\mathbf{t} = (x, y, z)^T$. Using this representation, the robot-world/hand-eye calibration problem can be posed as

$$\begin{pmatrix} \mathbf{R}_{\mathbf{A}_j} & \mathbf{t}_{\mathbf{A}_j} \\ 0 & 1 \end{pmatrix}\begin{pmatrix} \mathbf{R}_{\mathbf{X}} & \mathbf{t}_X \\ 0 & 1 \end{pmatrix} = \begin{pmatrix} \mathbf{R}_{\mathbf{Y}} & \mathbf{t}_Y \\ 0 & 1 \end{pmatrix}\begin{pmatrix} \mathbf{R}_{\mathbf{B}_j} & \mathbf{t}_{\mathbf{B}_j} \\ 0 & 1 \end{pmatrix}$$

which can be split into its orientational component

$$\mathbf{R}_{\mathbf{A}_j}\mathbf{R}_{\mathbf{X}} = \mathbf{R}_{\mathbf{Y}}\mathbf{R}_{\mathbf{B}_j} \quad (1)$$

and positional component

$$\mathbf{R}_{\mathbf{A}_j}\mathbf{t}_X + \mathbf{t}_{\mathbf{A}_j} = \mathbf{R}_{\mathbf{Y}}\mathbf{t}_{\mathbf{B}_j} + \mathbf{t}_Y \quad (2)$$

There have been many solutions to the robot-world/hand-eye calibration problem $\mathbf{A}_j\mathbf{X} = \mathbf{Y}\mathbf{B}_j$ as described in Refs. [1,2]. There, it is shown that the solutions can be split into two categories: iterative and closed-form. The iterative solutions [2–7] are generally very accurate when compared to the closed-form solutions. However, they are based on numerical techniques that can be slow and are dependent on initial conditions. In contrast, the closed-form solutions [4,7–10] are fast and are often used to bootstrap the iterative methods. For this paper, we will concentrate on solutions that are closed-form; i.e., the separable closed-form solutions, which solve the orientational component before solving the positional

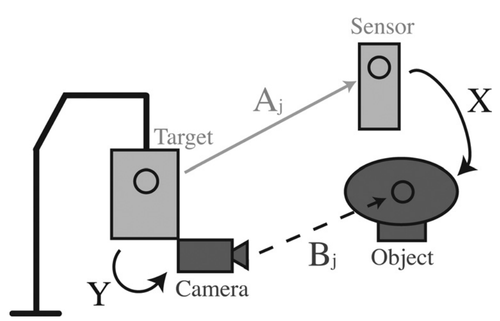

Fig. 1 Experimental setup consisting of two systems: a computer vision system and a precise sensor system considered ground truth

Contributed by the Mechanisms and Robotics Committee of ASME for publication in the JOURNAL OF MECHANISMS AND ROBOTICS. Manuscript received September 1, 2012; final manuscript received April 29, 2013; published online June 24, 2013. Assoc. Editor: J. M. Selig.

component, and the simultaneous closed-form solutions, which solve the orientational component and positional component at the same time. Many of these solutions are based on the closed-form solutions of the related hand-eye calibration problem $\mathbf{A}_j\mathbf{X} = \mathbf{X}\mathbf{B}_j$, which are formulated using either angle-axis formulations for rotations [11–13], Lie group theory [14], quaternions [15–21], screw theory [22], or Kronecker products [23].

Historically, the separable solutions to the robot-world/hand-eye calibration problem are formulated using quaternions [4,8]. These quaternion solutions are clean and efficient but can have stability issues as will be discussed in Sec. 5. In addition, errors computed from first solving the orientational component can get passed to the positional component. Simultaneous solutions do not have this problem; however, the optimal orientations ($\mathbf{R_X}$ and $\mathbf{R_Y}$) that are calculated may be negatively influenced by noise from the positional component [21]. Furthermore, simultaneous solutions may not live in the actual search space of possible applicable solutions [23]. For example, Li et al. [9] formulate a simultaneous solution to the robot-world/hand-eye calibration problem using the Kronecker product, which follows the methodology of solving the hand-eye calibration problem of Andreff et al. [23]. The resulting solution for the optimal orientations ($\mathbf{R_X}$ and $\mathbf{R_Y}$) may not necessarily be rotation matrices. Li et al. suggest calculating the best orthogonal approximation to guarantee a rotation. However, they do not update the positional approximation ($\mathbf{t}_X$ and $\mathbf{t}_Y$) after. This can lead to errors in the optimal positional approximation as will be shown in Sec. 5. In this paper, we create a stable separable closed-form solution that combines the quaternion work of [4,8] with the Kronecker work of [9,23]. Though this method is an example of a separable closed-form solution and thus suffers from the problem that errors obtained from first calculating the orientational component get passed to the positional component, the resulting positional errors may be less than the simultaneous methods. Examples of this phenomena will be shown in Sec. 5. For completeness, a full mathematical analysis of the problem, which includes minimal requirements to find a closed-form solution using the Kronecker product that were not discussed in Ref. [9], will also be presented. It should be noted that this analysis was inspired by the proofs shown in Refs. [4,8] that solved $\mathbf{A}_j\mathbf{X} = \mathbf{Y}\mathbf{B}_j$ using quaternions and in Ref. [23] that solved $\mathbf{A}_j\mathbf{X} = \mathbf{X}\mathbf{B}_j$ using the Kronecker product.

This paper is organized as followed: Sec. 2 will give qualifications and methodology for calculating the optimal rotations $\mathbf{R_Y}$ and $\mathbf{R_X}$, Sec. 3 will give qualifications and methodology for calculating the optimal translations $\mathbf{t}_Y$ and $\mathbf{t}_X$, Sec. 4 will describe error metrics, and Sec. 5 will describe experiments illustrating the effectiveness of the Kronecker product for solving the robot-world/hand-eye calibration problem. Here, $\|\cdot\|$ denotes the Frobenius norm, so

$$\|\mathbf{A}\| = \sqrt{\operatorname{tr}(\mathbf{A}\mathbf{A}^T)} = \sqrt{\operatorname{tr}(\mathbf{A}^T\mathbf{A})}$$

where ^{T} denotes the transpose operator and tr() denotes the matrix trace operation. The determinant of a matrix $\mathbf{A}$ is represented as $\det(\mathbf{A})$, vectorizing a matrix $\mathbf{A}$ column-wise is represented as $\operatorname{vec}(\mathbf{A})$, and the symbol $\otimes$ denotes the Kronecker product. Here, the Kronecker product of an $m \times n$ matrix $\mathbf{A}$ with a $p \times q$ matrix $\mathbf{B}$ is defined as the $mp \times nq$ matrix

$$\mathbf{A} \otimes \mathbf{B} = \begin{pmatrix} a_{11}\mathbf{B} & \cdots & a_{1n}\mathbf{B} \\ \vdots & \ddots & \vdots \\ a_{m1}\mathbf{B} & \cdots & a_{mn}\mathbf{B} \end{pmatrix}$$

Some properties of the Kronecker product that will be useful in the proofs of this paper are

(1) $(\mathbf{A} \otimes \mathbf{B})^{-1} = \mathbf{A}^{-1} \otimes \mathbf{B}^{-1}$
(2) $(\mathbf{A} \otimes \mathbf{B})^T = \mathbf{A}^T \otimes \mathbf{B}^T$
(3) $(\mathbf{A} \otimes \mathbf{B})(\mathbf{C} \otimes \mathbf{D}) = \mathbf{AC} \otimes \mathbf{BD}$
(4) If $\mathbf{A}$ is orthogonal and $\mathbf{B}$ is orthogonal, then their Kronecker product $\mathbf{A} \otimes \mathbf{B}$ is also orthogonal.

for matrices $\mathbf{A}$, $\mathbf{B}$, $\mathbf{C}$, and $\mathbf{D}$ of appropriate degree [24].

2 Finding $\mathbf{R_Y}$ and $\mathbf{R_X}$

This section presents the methodology and qualifications for obtaining a unique solution for $\mathbf{R_Y}$ and $\mathbf{R_X}$. To begin notice that the orientational component

$$\mathbf{R}_{\mathbf{A}_j}\mathbf{R_X} = \mathbf{R_Y}\mathbf{R}_{\mathbf{B}_j}$$

is equivalent to

$$\mathbf{R}_{\mathbf{A}_j}\mathbf{R_X}\mathbf{R}_{\mathbf{B}_j}^T = \mathbf{R_Y}$$

since $\mathbf{R}_{\mathbf{B}_j}$ is an orthogonal matrix. Therefore, the orientational component (1) can be represented as either

$$\begin{aligned} (\mathbf{R}_{\mathbf{B}_j} \otimes \mathbf{R}_{\mathbf{A}_j})\operatorname{vec}(\mathbf{R_X}) - \operatorname{vec}(\mathbf{R_Y}) &= 0 \\ \begin{pmatrix} -\mathbf{I} & \mathbf{R}_{\mathbf{B}_j} \otimes \mathbf{R}_{\mathbf{A}_j} \end{pmatrix} \begin{pmatrix} \operatorname{vec}(\mathbf{R_Y}) \\ \operatorname{vec}(\mathbf{R_X}) \end{pmatrix} &= 0 \end{aligned} \quad (3)$$

Here, we use the fact that if $\mathbf{AXB} = \mathbf{C}$ for unknown matrix $\mathbf{X}$, then the problem can be rewritten as a linear system

$$(\mathbf{B}^T \otimes \mathbf{A})\operatorname{vec}(\mathbf{X}) = \operatorname{vec}(\mathbf{AXB}) = \operatorname{vec}(\mathbf{C})$$

Note that once the rotation matrix $\mathbf{R_Y}$ is known, the positional component (2) can be represented as the linear system

$$\begin{pmatrix} \mathbf{I} & -\mathbf{R}_{\mathbf{A}_j} \end{pmatrix} \begin{pmatrix} \mathbf{t}_Y \\ \mathbf{t}_X \end{pmatrix} = \mathbf{t}_{\mathbf{A}_j} - \mathbf{R_Y}\mathbf{t}_{\mathbf{B}_j} \quad (4)$$

The following lemma will be useful in characterizing a unique solution for $\mathbf{R_Y}$ and $\mathbf{R_X}$.

LEMMA 2.1. *The matrices* $\mathbf{R}_{\mathbf{B}_j}^T\mathbf{R}_{\mathbf{B}_k}$ *and* $\mathbf{R}_{\mathbf{A}_j}^T\mathbf{R}_{\mathbf{A}_k}$ *have the same eigenvalues for* $j, k = 1, 2,\ldots, n$. *Furthermore, these eigenvalues can be represented as* $\{1, e^{i\theta}, e^{-i\theta}\}$.

Proof. We assume that

$$\mathbf{R}_{\mathbf{A}_j}\mathbf{R_X} = \mathbf{R_Y}\mathbf{R}_{\mathbf{B}_j} \Leftrightarrow \mathbf{R}_{\mathbf{A}_j}\mathbf{R_X}\mathbf{R}_{\mathbf{B}_j}^T = \mathbf{R_Y}$$

for $j, k = 1, 2,\ldots, n$. But, then

$$\mathbf{R}_{\mathbf{A}_j}\mathbf{R_X}\mathbf{R}_{\mathbf{B}_j}^T = \mathbf{R_Y} = \mathbf{R}_{\mathbf{A}_k}\mathbf{R_X}\mathbf{R}_{\mathbf{B}_k}^T \Rightarrow \mathbf{R}_{\mathbf{A}_k}^T\mathbf{R}_{\mathbf{A}_j} = \mathbf{R_X}\mathbf{R}_{\mathbf{B}_k}^T\mathbf{R}_{\mathbf{B}_j}\mathbf{R_X}^T$$

Therefore, $\mathbf{R}_{\mathbf{B}_k}^T\mathbf{R}_{\mathbf{B}_j}$ and $\mathbf{R}_{\mathbf{A}_k}^T\mathbf{R}_{\mathbf{A}_j}$ are similar matrices and thus have the same eigenvalues. Furthermore, since both of these matrices are rotations their eigenvalues can be represented as $\{1 e^{i\theta} e^{-i\theta}\}$.

Using the above lemma, the minimum number of pose measurement can now be given. We should note that these qualifications are similar to the qualifications of uniqueness shown for the quaternion method of [8]. However, the proofs here are derived using the Kronecker product instead of quaternions.

THEOREM 2.2. *The minimum number* n *of pose measurements necessary to obtain a unique solution to linear system (3) is* $n = 3$.

Proof. Consider the case where $n = 2$. Then the linear system (3) becomes

$$\begin{pmatrix} -\mathbf{I} & \mathbf{R}_{\mathbf{B}_1} \otimes \mathbf{R}_{\mathbf{A}_1} \\ -\mathbf{I} & \mathbf{R}_{\mathbf{B}_2} \otimes \mathbf{R}_{\mathbf{A}_2} \end{pmatrix} \begin{pmatrix} \operatorname{vec}(\mathbf{R_Y}) \\ \operatorname{vec}(\mathbf{R_X}) \end{pmatrix} = \begin{pmatrix} 0 \\ 0 \end{pmatrix}$$

which clearly is a square system. However, the dimension of the nullspace is at least three. This can be seen by first noticing

$$\operatorname{rank}\begin{pmatrix} -\mathbf{I} & \mathbf{R}_{\mathbf{B}_1}\otimes\mathbf{R}_{\mathbf{A}_1} \\ -\mathbf{I} & \mathbf{R}_{\mathbf{B}_2}\otimes\mathbf{R}_{\mathbf{A}_2}\end{pmatrix} = \operatorname{rank}\begin{pmatrix} -\mathbf{I} & \mathbf{R}_{\mathbf{B}_1}\otimes\mathbf{R}_{\mathbf{A}_1} \\ 0 & \mathbf{R}_{\mathbf{B}_1}\otimes\mathbf{R}_{\mathbf{A}_1} - \mathbf{R}_{\mathbf{B}_2}\otimes\mathbf{R}_{\mathbf{A}_2}\end{pmatrix}$$

by elementary matrix row operations. Hence, the resulting matrix is block-triangular and the

$$\begin{aligned}&\operatorname{rank}(\mathbf{R}_{\mathbf{B}_1}\otimes\mathbf{R}_{\mathbf{A}_1} - \mathbf{R}_{\mathbf{B}_2}\otimes\mathbf{R}_{\mathbf{A}_2})\\ &= \operatorname{rank}\Big((\mathbf{R}_{\mathbf{B}_1}\otimes\mathbf{R}_{\mathbf{A}_1})(\mathbf{I} - \mathbf{R}_{\mathbf{B}_1}^T\mathbf{R}_{\mathbf{B}_2}\otimes\mathbf{R}_{\mathbf{A}_1}^T\mathbf{R}_{\mathbf{A}_2})\Big)\\ &= \operatorname{rank}\Big(\mathbf{I} - \mathbf{R}_{\mathbf{B}_1}^T\mathbf{R}_{\mathbf{B}_2}\otimes\mathbf{R}_{\mathbf{A}_1}^T\mathbf{R}_{\mathbf{A}_2})\Big) \le 6\end{aligned}$$

This is a consequence of the previous lemma: since $\mathbf{R}_{\mathbf{B}_1}^T\mathbf{R}_{\mathbf{B}_2}$ and $\mathbf{R}_{\mathbf{A}_1}^T\mathbf{R}_{\mathbf{A}_2}$ have similar eigenvalues $\{1, e^{i\theta}, e^{-i\theta}\}$, at least three of the eigenvalues of $\mathbf{R}_{\mathbf{B}_1}^T\mathbf{R}_{\mathbf{B}_2}\otimes\mathbf{R}_{\mathbf{A}_1}^T\mathbf{R}_{\mathbf{A}_2}$ are 1. Therefore,

$$\operatorname{rank}(\mathbf{R}_{\mathbf{B}_1}\otimes\mathbf{R}_{\mathbf{A}_1} - \mathbf{R}_{\mathbf{B}_2}\otimes\mathbf{R}_{\mathbf{A}_2}) \le 6.$$

Consequently, the dimension of the nullspace is greater than one, and thus the number of pose measurements $n \ge 3$.

Even when $n=3$ there are situations when the linear system does not have a unique solution as illustrated in the following theorem.

THEOREM 2.3. *Assume $n=3$. If the principal axes (up to sign) for $\mathbf{R}_{\mathbf{A}_2}^T\mathbf{R}_{\mathbf{A}_1}$ and $\mathbf{R}_{\mathbf{A}_3}^T\mathbf{R}_{\mathbf{A}_1}$ are not equal, then the linear system (3) has a unique solution.*

Proof. For $n=3$ the linear system (3) becomes

$$\begin{aligned}(\mathbf{R}_{\mathbf{B}_1}\otimes\mathbf{R}_{\mathbf{A}_1})\operatorname{vec}(\mathbf{R}_\mathbf{X}) - \operatorname{vec}(\mathbf{R}_\mathbf{Y}) = 0\\ (\mathbf{R}_{\mathbf{B}_2}\otimes\mathbf{R}_{\mathbf{A}_2})\operatorname{vec}(\mathbf{R}_\mathbf{X}) - \operatorname{vec}(\mathbf{R}_\mathbf{Y}) = 0\\ (\mathbf{R}_{\mathbf{B}_3}\otimes\mathbf{R}_{\mathbf{A}_3})\operatorname{vec}(\mathbf{R}_\mathbf{X}) - \operatorname{vec}(\mathbf{R}_\mathbf{Y}) = 0\end{aligned}$$

which implies

$$\begin{aligned}(\mathbf{R}_{\mathbf{B}_1}\otimes\mathbf{R}_{\mathbf{A}_1})\operatorname{vec}(\mathbf{R}_\mathbf{X}) &= (\mathbf{R}_{\mathbf{B}_2}\otimes\mathbf{R}_{\mathbf{A}_2})\operatorname{vec}(\mathbf{R}_\mathbf{X})\\ &= (\mathbf{R}_{\mathbf{B}_3}\otimes\mathbf{R}_{\mathbf{A}_3})\operatorname{vec}(\mathbf{R}_\mathbf{X})\end{aligned}$$

But, then

$$\begin{aligned}(\mathbf{R}_{\mathbf{B}_1}^T\mathbf{R}_{\mathbf{B}_2}\otimes\mathbf{R}_{\mathbf{A}_1}^T\mathbf{R}_{\mathbf{A}_2})\operatorname{vec}(\mathbf{R}_\mathbf{X}) = \operatorname{vec}(\mathbf{R}_\mathbf{X})\\ (\mathbf{R}_{\mathbf{B}_1}^T\mathbf{R}_{\mathbf{B}_3}\otimes\mathbf{R}_{\mathbf{A}_1}^T\mathbf{R}_{\mathbf{A}_3})\operatorname{vec}(\mathbf{R}_\mathbf{X}) = \operatorname{vec}(\mathbf{R}_\mathbf{X})\end{aligned}$$

which is equivalent to finding the nullspace of

$$\begin{pmatrix}\mathbf{I} - (\mathbf{R}_{\mathbf{B}_1}^T\mathbf{R}_{\mathbf{B}_2}\otimes\mathbf{R}_{\mathbf{A}_1}^T\mathbf{R}_{\mathbf{A}_2})\\ \mathbf{I} - (\mathbf{R}_{\mathbf{B}_1}^T\mathbf{R}_{\mathbf{B}_3}\otimes\mathbf{R}_{\mathbf{A}_1}^T\mathbf{R}_{\mathbf{A}_3})\end{pmatrix}\operatorname{vec}(\mathbf{R}_\mathbf{X}) = 0 \tag{5}$$

This problem appears in the work of Ref. [23] where they are searching for the solution of the similar problem $\mathbf{R}_A\mathbf{R}_\mathbf{X} = \mathbf{R}_\mathbf{X}\mathbf{R}_B$. In this work, they reformulate the problem as

$$\begin{pmatrix}\mathbf{I} - (\mathbf{R}_{\mathbf{B}_1}\otimes\mathbf{R}_{\mathbf{A}_1})\\ \mathbf{I} - (\mathbf{R}_{\mathbf{B}_2}\otimes\mathbf{R}_{\mathbf{A}_2})\end{pmatrix}\operatorname{vec}(\mathbf{R}_\mathbf{X}) = 0$$

and show that a unique solution exists only if the principal axes of $\mathbf{R}_{\mathbf{A}_1}$ and $\mathbf{R}_{\mathbf{A}_2}$ are nonparallel. For problem (5), this is equivalent to stating that the principal axes of $\mathbf{R}_{\mathbf{A}_1}^T\mathbf{R}_{\mathbf{A}_2}$ and $\mathbf{R}_{\mathbf{A}_1}^T\mathbf{R}_{\mathbf{A}_3}$ are not equal (up to sign).

We now concentrate on finding an efficient unique solution for linear system (3). For $n \ge 3$, linear system (3) becomes rectangular and therefore the nullspace for the corresponding normal equation

$$\begin{pmatrix} n\mathbf{I} & -\sum_{j=1}^n \mathbf{R}_{\mathbf{B}_j}\otimes\mathbf{R}_{\mathbf{A}_j}\\ -\sum_{j=1}^n \mathbf{R}_{\mathbf{B}_j}^T\otimes\mathbf{R}_{\mathbf{A}_j}^T & n\mathbf{I}\end{pmatrix}\begin{pmatrix}\operatorname{vec}(\mathbf{R}_\mathbf{Y})\\ \operatorname{vec}(\mathbf{R}_\mathbf{X})\end{pmatrix} = \begin{pmatrix}0\\0\end{pmatrix} \tag{6}$$

has to be considered. Note that the normal equation for a linear system $\mathbf{A}\mathbf{x} = \mathbf{b}$ is defined as $\mathbf{A}^T\mathbf{A}\mathbf{x} = \mathbf{A}^T\mathbf{b}$.

THEOREM 2.4. *The solutions $vec(\mathbf{R}_\mathbf{Y})$ and $vec(\mathbf{R}_\mathbf{X})$ of the linear system (6) are proportional to the left singular vector $\mathbf{u}_n$ and right singular vector $\mathbf{v}_n$ corresponding to the singular value, n, of*

$$\mathbf{K} = \sum_{j=1}^n \mathbf{R}_{\mathbf{B}_j}\otimes\mathbf{R}_{\mathbf{A}_j}$$

respectively. The resulting $\mathbf{R}_\mathbf{X}$ and $\mathbf{R}_\mathbf{Y}$ can be calculated as

$$\begin{aligned}\mathbf{R}_\mathbf{X} = \alpha\mathbf{V}_X\\ \mathbf{R}_\mathbf{Y} = \beta\mathbf{V}_Y\end{aligned}$$

where $\mathbf{V}_X = \operatorname{vec}^{-1}(\mathbf{v}_n)$, $\mathbf{V}_Y = \operatorname{vec}^{-1}(\mathbf{u}_n)$, and

$$\begin{aligned}\alpha = \operatorname{sign}(\mathbf{V}_X)\det(\mathbf{V}_X)^{-1/3}\\ \beta = \operatorname{sign}(\mathbf{V}_Y)\det(\mathbf{V}_Y)^{-1/3}\end{aligned}$$

Proof. Breaking up the linear system (6) leads to two equations:

$$\begin{aligned}n\ \operatorname{vec}(\mathbf{R}_\mathbf{Y}) - \mathbf{K}\ \operatorname{vec}(\mathbf{R}_\mathbf{X}) = 0\\ -\mathbf{K}^T\ \operatorname{vec}(\mathbf{R}_\mathbf{Y}) + n\ \operatorname{vec}(\mathbf{R}_\mathbf{X}) = 0\end{aligned}$$

Solving the first equation yields

$$\operatorname{vec}(\mathbf{R}_\mathbf{Y}) = \frac{1}{n}\mathbf{K}\ \operatorname{vec}(\mathbf{R}_\mathbf{X})$$

and substituting this expression into the second equation yields

$$n^2\operatorname{vec}(\mathbf{R}_\mathbf{X}) = \mathbf{K}^T\mathbf{K}\ \operatorname{vec}(\mathbf{R}_\mathbf{X})$$

Similarly, we can show that

$$n^2\operatorname{vec}(\mathbf{R}_\mathbf{Y}) = \mathbf{K}\mathbf{K}^T\ \operatorname{vec}(\mathbf{R}_\mathbf{Y})$$

Therefore, $\operatorname{vec}(\mathbf{R}_\mathbf{X})$ is proportional to the eigenvector corresponding to the eigenvalue n^2 of $\mathbf{K}^T\mathbf{K}$ and $\operatorname{vec}(\mathbf{R}_\mathbf{Y})$ is proportional to the eigenvector corresponding the to eigenvalue of n^2 of $\mathbf{K}\mathbf{K}^T$. These vectors can efficiently be computed by taking the singular value decomposition of $\mathbf{K}$. Specifically, $\operatorname{vec}(\mathbf{R}_\mathbf{Y})$ is proportional to the left singular vector $\mathbf{u}_n$ and $\operatorname{vec}(\mathbf{R}_\mathbf{X})$ is proportional to the right singular vector $\mathbf{v}_n$ corresponding to the singular value n. Let $\mathbf{V}_Y = \operatorname{vec}^{-1}(\mathbf{u}_n)$ and $\mathbf{V}_X = \operatorname{vec}^{-1}(\mathbf{v}_n)$. The proportionality constants can be determined by noting that $\det(\mathbf{R}_\mathbf{X}) = 1 = \det(\mathbf{R}_\mathbf{Y})$, since $\mathbf{R}_\mathbf{X}$ and $\mathbf{R}_\mathbf{Y}$ are rotation matrices. Therefore, since

$$\begin{aligned}\alpha\mathbf{V}_X = \mathbf{R}_\mathbf{X}\\ \beta\mathbf{V}_Y = \mathbf{R}_\mathbf{Y}\end{aligned}$$

the proportionality constants

$$\begin{aligned}\alpha = \operatorname{sign}(\mathbf{V}_X)\det(\mathbf{V}_X)^{-1/3}\\ \beta = \operatorname{sign}(\mathbf{V}_Y)\det(\mathbf{V}_Y)^{-1/3}\end{aligned}$$

Here, we use the property that $\det(\alpha\mathbf{X}) = \alpha^3\det(\mathbf{X})$ for given scalar α and 3×3 matrix $\mathbf{X}$.

In practice, the method above may not give accurate solutions due to noise. The method above guarantees that the computed $\mathbf{R}_\mathbf{X}$ and $\mathbf{R}_\mathbf{Y}$ have determinant 1. However, the orthogonality of the matrices $\mathbf{R}_\mathbf{X}$ and $\mathbf{R}_\mathbf{Y}$ computed from the method may be lost due to noise. Therefore, it may be beneficial to re-orthogonalize the computed matrices to guarantee that they are indeed rotations. In addition, noise in the data may make it difficult to find the eigenvector corresponding to a specific value. As a result, the next theorem proves that n^2 is the largest possible eigenvalue for $\mathbf{K}^T\mathbf{K}$, and hence n is the largest singular value of $\mathbf{K}$. Therefore, in practice instead of searching for the singular vectors corresponding to the singular value n, one should search for singular vectors corresponding to the largest singular value of $\mathbf{K}$.

THEOREM 2.5. *The largest possible eigenvalue of* $\mathbf{K}^T\mathbf{K}$ *is* n^2.

Proof. To show that n^2 is the largest possible eigenvalue of $\mathbf{K}^T\mathbf{K}$, first note that this is a real symmetric matrix. Consequently, by the Rayleigh quotient

$$\mathbf{x}^T\mathbf{K}^T\mathbf{K}\mathbf{x} = \lambda_{\max}$$

if $\mathbf{x}$ is a unit eigenvector corresponding to the largest eigenvalue $\lambda_{\max}$ of $\mathbf{K}^T\mathbf{K}$. But,

$$\begin{aligned}\lambda_{\max} &= \mathbf{x}^T\mathbf{K}^T\mathbf{K}\mathbf{x} \\ &= \sum_{j=1}^{n}\sum_{k=1}^{n}\mathbf{x}^T\left(\mathbf{R}_{\mathbf{B}_j}^T\mathbf{R}_{\mathbf{B}_k}\otimes\mathbf{R}_{\mathbf{A}_j}^T\mathbf{R}_{\mathbf{A}_k}\right)\mathbf{x} \\ &= \sum_{j=1}^{n}\sum_{k=1}^{n}\mathbf{x}^T\mathbf{y}_{\{j,k\}} \le n^2\end{aligned}$$

where

$$\mathbf{y}_{\{j,k\}} = \left(\mathbf{R}_{\mathbf{B}_j}^T\mathbf{R}_{\mathbf{B}_k}\otimes\mathbf{R}_{\mathbf{A}_j}^T\mathbf{R}_{\mathbf{A}_k}\right)\mathbf{x}$$

However, in the last theorem it was shown that n is a singular value for $\mathbf{K}$. Thus, n^2 is an eigenvalue of $\mathbf{K}^T\mathbf{K}$. Moreover,

$$\lambda_{\max} = n^2$$

Note in this proof we used the fact that $\mathbf{y}_{\{j,k\}}$ is a unit vector since $\mathbf{R}_{\mathbf{B}_j}^T\mathbf{R}_{\mathbf{B}_k}\otimes\mathbf{R}_{\mathbf{A}_j}^T\mathbf{R}_{\mathbf{A}_k}$ is an orthogonal matrix and hence preserves length. Therefore, $\mathbf{x}^T\mathbf{y}_{\{jk.\}} \le 1$.

3 Finding $\mathbf{t}_x$ and $\mathbf{t}_y$

Once $\mathbf{R_Y}$ is calculated with the method outlined from Sec. 2, in THEOREM 2.4 $\mathbf{t}_X$ and $\mathbf{t}_Y$ can be calculated. Specifically, $\mathbf{t}_X$ and $\mathbf{t}_Y$ is the solution to the linear system (4):

$$\begin{pmatrix}\mathbf{I} & -\mathbf{R}_{\mathbf{A}_j}\end{pmatrix}\begin{pmatrix}\mathbf{t}_Y \\ \mathbf{t}_X\end{pmatrix} = \mathbf{t}_{\mathbf{A}_j} - \mathbf{R_Y}\mathbf{t}_{\mathbf{B}_j}$$

Clearly, multiple measurements are necessary to obtain a unique solution for this problem. The following will give qualifications for uniqueness. It should be noted that the results of this section are similar to the results of solving $\mathbf{AX} = \mathbf{YB}$ using quaternions shown in Ref. [8].

THEOREM 3.1. *The minimum number n of pose measurements necessary to obtain a unique solution to linear system (4) is* $n = 3$.

Proof. Consider the case where $n = 2$. Then the linear system (4) becomes

$$\begin{pmatrix}\mathbf{I} & -\mathbf{R}_{\mathbf{A}_1} \\ \mathbf{I} & -\mathbf{R}_{\mathbf{A}_2}\end{pmatrix}\begin{pmatrix}\mathbf{t}_Y \\ \mathbf{t}_X\end{pmatrix} = \begin{pmatrix}\mathbf{t}_{\mathbf{A}_1} - \mathbf{R_Y}\mathbf{t}_{\mathbf{B}_1} \\ \mathbf{t}_{\mathbf{A}_2} - \mathbf{R_Y}\mathbf{t}_{\mathbf{B}_2}\end{pmatrix}$$

which clearly is a square system. Therefore, uniqueness of the solution is dependent on the rank of the matrix

$$\begin{pmatrix}\mathbf{I} & -\mathbf{R}_{\mathbf{A}_1} \\ \mathbf{I} & -\mathbf{R}_{\mathbf{A}_2}\end{pmatrix}$$

By elementary row operations

$$\operatorname{rank}\begin{pmatrix}\mathbf{I} & -\mathbf{R}_{\mathbf{A}_1} \\ \mathbf{I} & -\mathbf{R}_{\mathbf{A}_2}\end{pmatrix} = \operatorname{rank}\begin{pmatrix}\mathbf{I} & -\mathbf{R}_{\mathbf{A}_1} \\ 0 & \mathbf{R}_{\mathbf{A}_1} - \mathbf{R}_{\mathbf{A}_2}\end{pmatrix}$$

which is a triangular system. Hence, the rank of the original matrix is dependent on the rank of

$$\mathbf{R}_{\mathbf{A}_1} - \mathbf{R}_{\mathbf{A}_2} = \mathbf{R}_{\mathbf{A}_1}\left(\mathbf{I} - \mathbf{R}_{\mathbf{A}_1}^T\mathbf{R}_{\mathbf{A}_2}\right)$$

which is clearly rank-deficient since at least one eigenvalue of the rotation matrix $\mathbf{R}_{\mathbf{A}_1}^T\mathbf{R}_{\mathbf{A}_2}$ has to be 1. Thus, $n \ge 3$.

THEOREM 3.2. *Assume* $n = 3$. *If the principal axes (up to sign) of* $\mathbf{R}_{\mathbf{A}_j}^T\mathbf{R}_{\mathbf{A}_k}$ *are not equal to the principal axes of* $\mathbf{R}_{\mathbf{A}_j}^T\mathbf{R}_{\mathbf{A}_\ell}$ *for* $j \ne k \ne \ell$, *then the linear system (4) has a unique solution.*

Proof. Consider the nullspace of the matrix from linear system (4)

$$\begin{pmatrix}\mathbf{I} & -\mathbf{R}_{\mathbf{A}_1} \\ \mathbf{I} & -\mathbf{R}_{\mathbf{A}_2} \\ \mathbf{I} & -\mathbf{R}_{\mathbf{A}_3}\end{pmatrix}\begin{pmatrix}\mathbf{t}_Y \\ \mathbf{t}_X\end{pmatrix} = 0$$

Thus, for $j = 1, 2, 3$

$$\mathbf{R}_{\mathbf{A}_j}\mathbf{t}_X = \mathbf{t}_Y$$

But, then

$$\mathbf{R}_{\mathbf{A}_j}^T\mathbf{R}_{\mathbf{A}_k}\mathbf{t}_X = \mathbf{R}_{\mathbf{A}_j}^T\mathbf{R}_{\mathbf{A}_\ell}\mathbf{t}_X = \mathbf{t}_X$$

which implies that $\mathbf{t}_X = 0$ or $\mathbf{t}_X$ is the principal axis for both $\mathbf{R}_{\mathbf{A}_j}^T\mathbf{R}_{\mathbf{A}_k}$ and $\mathbf{R}_{\mathbf{A}_j}^T\mathbf{R}_{\mathbf{A}_\ell}$. Since we assumed that the latter is not possible, then $\mathbf{t}_X = 0$ which implies that $\mathbf{t}_Y = 0$ Thus, linear system (4) has a unique solution.

4 Error Metrics

It is often beneficial to understand how well a given $\mathbf{X}$ (or $\mathbf{R_X}$ and $\mathbf{t}_X$) and $\mathbf{Y}$ (or $\mathbf{R_Y}$ and $\mathbf{t}_Y$) fit the data for evaluation purposes. In order to create error metrics, we will split the problem setup into its orientational component (1)

$$\mathbf{R}_{\mathbf{A}_j}\mathbf{R_X} = \mathbf{R_Y}\mathbf{R}_{\mathbf{B}_j}$$

and positional component (2)

$$\mathbf{R}_{\mathbf{A}_j}\mathbf{t}_X + \mathbf{t}_{\mathbf{A}_j} = \mathbf{R_Y}\mathbf{t}_{\mathbf{B}_j} + \mathbf{t}_Y$$

Using these descriptions, an error metric for the orientational component (1) and positional component (2) can be formulated. This formulation is inspired by the error metrics of the author's earlier work [25]. Specifically, the error metric for the orientational component (1) can be formulated as

$$\begin{aligned}&\|\mathbf{R}_{\mathbf{A}_j}\mathbf{R_X} - \mathbf{R_Y}\mathbf{R}_{\mathbf{B}_j}\|^2 \\ &\quad = \|\mathbf{R}_{\mathbf{A}_j}\mathbf{R_X}\|^2 - 2\operatorname{tr}\left(\mathbf{R}_{\mathbf{A}_j}\mathbf{R_X}\left(\mathbf{R_Y}\mathbf{R}_{\mathbf{B}_j}\right)^T\right) + \|\mathbf{R_Y}\mathbf{R}_{\mathbf{B}_j}\|^2 \\ &\quad = 6 - 2\operatorname{tr}\left(\mathbf{R}_{\mathbf{A}_j}\mathbf{R_X}\left(\mathbf{R_Y}\mathbf{R}_{\mathbf{B}_j}\right)^T\right) \\ &\quad = 6 - 2(1 + 2\cos\theta) \le 8\end{aligned}$$

since $\|\mathbf{R}\|^2 = 3$ and $\operatorname{tr}(\mathbf{R}) = 1 + 2\cos\theta$ for any rotation matrix $\mathbf{R}$ with eigenvalues $\{1, \cos\theta \pm i\sin\theta\}$. Therefore, if $\theta = 0$, then $6 - 2(1 + 2\cos\theta) = 6 - 2(3) = 0$, whereas if $\theta = \pi$, then $6 - 2(1 + 2\cos\theta) = 6 - 2(-1) = 8$. Hence, a metric or *percentage of accuracy* to evaluate the orientation for a given $\mathbf{R_X}$ and $\mathbf{R_Y}$ can be calculated as

$$0 \le 1 - \frac{1}{8}\|\mathbf{R}_{\mathbf{A}_j}\mathbf{R_X} - \mathbf{R_Y}\mathbf{R}_{\mathbf{B}_j}\|^2 \le 1$$

A metric for the positional component (2) can be calculated in a similar way by considering how close

$$\mathbf{R}_{\mathbf{A}_j}\mathbf{t}_X + \mathbf{t}_{\mathbf{A}_j} \text{ is to } \mathbf{R}_\mathbf{Y}\mathbf{t}_{\mathbf{B}_j} + \mathbf{t}_Y$$

The dot product of the normalized vectors, i.e.,

$$0 \le \left| \frac{\left(\mathbf{R}_{\mathbf{A}_j}\mathbf{t}_X + \mathbf{t}_{\mathbf{A}_j}\right)^T \left(\mathbf{R}_\mathbf{Y}\mathbf{t}_{\mathbf{B}_j} + \mathbf{t}_Y\right)}{\|\mathbf{R}_{\mathbf{A}_j}\mathbf{t}_X + \mathbf{t}_{\mathbf{A}_j}\|\|\mathbf{R}_\mathbf{Y}\mathbf{t}_{\mathbf{B}_j} + \mathbf{t}_Y\|} \right| \le 1$$

can be used to construct a metric or *percentage of accuracy* for this data. If the dot product of the vectors is 1, then the algorithm has 100% accuracy. A problem with this metric is that the scale of the vectors is not taken into consideration. Therefore, two vectors that are not exactly equal may exhibit 100% accuracy. For example, consider the vectors $\mathbf{x}$ and $\mathbf{y} = \lambda\mathbf{x}$ where the scaling term λ is any real number other than 1. The dot product of these normalized vectors would be 1 but $\mathbf{x} \neq \mathbf{y}$. Therefore, one may additionally want to compare the scale of

$$\left\| \left(\mathbf{R}_{\mathbf{A}_j}\mathbf{t}_X + \mathbf{t}_{\mathbf{A}_j}\right) - \left(\mathbf{R}_\mathbf{Y}\mathbf{t}_{\mathbf{B}_j} + \mathbf{t}_Y\right) \right\|$$

with the scale of the positional data $\mathbf{t}_{\mathbf{A}_j}$ and $\mathbf{t}_{\mathbf{B}_j}$ to determine the accuracy of the algorithm. Note that since this metric does not have an upper-bound, it may be difficult to compare the results from different setups as is possible with the first metric presented.

5 Experiments

5.1 Simulated Data In this section, the Kronecker method presented in this paper is compared with the Li et al. Kronecker method [9] and the Dornaika and Horaud closed-form quaternion method [4] on simulated data. The simulated data were constructed by first setting $\mathbf{A}_j$ as a random homogeneous matrix where the positional data $\mathbf{t}_{\mathbf{A}_j}$ are pseudorandom values drawn from the standard uniform distribution on the open interval (0, 1) for $j = 1, 2, \ldots, 20$. The corresponding

$$\mathbf{B}_j = \mathbf{Y}^{-1}\mathbf{A}_j\mathbf{X}$$

for random homogeneous matrices $\mathbf{X}$ and $\mathbf{Y}$. Noise was then added to the orientational component of $\mathbf{B}_j$ by setting the quaternion representation $\mathbf{q}_{\mathbf{B}_j}$ of $\mathbf{R}_{\mathbf{B}_j}$ to

$$\hat{\mathbf{q}}_{\mathbf{B}_j} = \frac{\mathbf{q}_{\mathbf{B}_j} + \eta\,\mathbf{n}_4}{\|\mathbf{q}_{\mathbf{B}_j} + \eta\,\mathbf{n}_4\|}$$

Here, η spans 20 equally spaced values between 0 and 0.25 and $\mathbf{n}_4$ is a four-dimensional vector of pseudorandom values drawn from the standard uniform distribution on the open interval (0,1). Note the positional data remained exact.

Figure 2 shows the average results over ten trials of the experiment with increasing η values. The rotation errors are described as

$$0 \le \|\mathbf{R} - \hat{\mathbf{R}}\| = \sqrt{6 - 2(1 + 2\cos\theta)} \le \sqrt{8}$$

where $\mathbf{R}$ is the original non-noisy rotation matrix and $\hat{\mathbf{R}}$ is the rotation matrix computed from each of the three methods. Here, θ describes the angle of rotation for the rotation matrix $\mathbf{R}\hat{\mathbf{R}}^T$. Notice that if $\mathbf{R} = \hat{\mathbf{R}}$, then $\mathbf{R}\hat{\mathbf{R}}^T = \mathbf{I}$ and the angle of rotation $\theta = 0$. Similarly, the position errors are described as

$$\|\mathbf{t} - \hat{\mathbf{t}}\|$$

where $\mathbf{t}$ is the original non-noisy position vector and $\hat{\mathbf{t}}$ is the position vector computed from each of the three methods. The Kronecker method presented in this paper is represented with circles, the Li et al. Kronecker method is described with triangles and the Dornaika and Horaud closed-form quaternion method is described with a solid line.

Generally, the results of the Kronecker method presented in this paper and the Dornaika and Horaud method are the same. However, there are a couple of peaks where the methods differ. This is a consequence of the nonuniqueness of the quaternion representation for rotation. Specifically, the Dornaika and Horaud method calculates the optimal orientations by forming a minimization problem under the assumption that

$$\mathbf{q}_{\mathbf{A}_j}\mathbf{q}_\mathbf{X} = \mathbf{q}_\mathbf{Y}\mathbf{q}_{\mathbf{B}_j}$$

However, since quaternions that represent rotation are sign invariant, this method can produce inaccurate results. For example, let the quaternion representation for

$$\mathbf{q}_\mathbf{A} = \left\{ \begin{pmatrix} 0.5959 \\ 0.1411 \\ 0.3562 \\ 0.7058 \end{pmatrix}, \begin{pmatrix} 0.1004 \\ 0.9834 \\ 0.1473 \\ 0.0337 \end{pmatrix}, \begin{pmatrix} 0.3101 \\ 0.6635 \\ 0.5309 \\ 0.4264 \end{pmatrix} \right\}$$

$$\mathbf{q}_\mathbf{B} = \left\{ \begin{pmatrix} 0.6359 \\ 0.5622 \\ 0.4566 \\ 0.2666 \end{pmatrix}, \begin{pmatrix} -0.7766 \\ -0.1562 \\ 0.4056 \\ 0.4560 \end{pmatrix}, \begin{pmatrix} 0.8277 \\ 0.5402 \\ -0.1499 \\ 0.0258 \end{pmatrix} \right\}$$

Then for the true $\mathbf{q}_\mathbf{X}$ and $\mathbf{q}_\mathbf{Y}$

$$\mathbf{q}_\mathbf{A}\mathbf{q}_\mathbf{X} = \left\{ \begin{pmatrix} 0.5599 \\ 0.5915 \\ 0.1721 \\ -0.5541 \end{pmatrix}, \begin{pmatrix} 0.0254 \\ 0.2290 \\ -0.8422 \\ -0.4874 \end{pmatrix}, \begin{pmatrix} 0.2343 \\ 0.6979 \\ -0.4156 \\ -0.5342 \end{pmatrix} \right\}$$

$$\mathbf{q}_\mathbf{Y}\mathbf{q}_\mathbf{B} = \left\{ \begin{pmatrix} 0.5599 \\ 0.5915 \\ 0.1721 \\ -0.5541 \end{pmatrix}, \begin{pmatrix} -0.0254 \\ -0.2290 \\ 0.8422 \\ 0.4874 \end{pmatrix}, \begin{pmatrix} 0.2343 \\ 0.6979 \\ -0.4156 \\ -0.5342 \end{pmatrix} \right\}$$

Notice that the second quaternion in each set have opposite signs. Thus, the Dornaika and Horaud method creates inaccurate results. Specifically, the quaternion representation for the results obtained from the Dornaika and Horaud method are

$$\mathbf{q}_\mathbf{X} = (-0.1981 \quad 0.5408 \quad -0.8172 \quad 0.0239)^T$$
$$\mathbf{q}_\mathbf{Y} = (-0.7639 \quad -0.0660 \quad 0.6339 \quad 0.1018)^T$$

whereas the true results and the one calculated using the Kronecker product method created in this paper are

$$\mathbf{q}_\mathbf{X} = (0.9118 \quad 0.3988 \quad 0.0454 \quad 0.0873)^T$$
$$\mathbf{q}_\mathbf{Y} = (0.3283 \quad 0.6154 \quad 0.3603 \quad 0.6194)^T$$

Figure 2 also illustrates the differences between the Kronecker method presented in this paper and the Li et al. Kronecker method. The $\mathbf{X}$ rotational errors are similar. However, the $\mathbf{Y}$ rotation errors of the Li et al. Kronecker method are slightly better than the errors of the Kronecker method presented in this paper, since their calculation includes the exact positional data. However, the positional errors vary drastically. This is a result of the Li et al. Kronecker method calculating $\mathbf{R}_\mathbf{X}, \mathbf{R}_\mathbf{Y}, \mathbf{t}_X$, and $\mathbf{t}_Y$ all in the same step. Due to noise, the $\mathbf{R}_\mathbf{X}$ and $\mathbf{R}_\mathbf{Y}$ calculated may not be accurate representations of rotation matrices and thus a further step has to be made which may cause discrepancies. However, the corresponding $\mathbf{t}_X$ and $\mathbf{t}_Y$ are not updated with the Li et al.

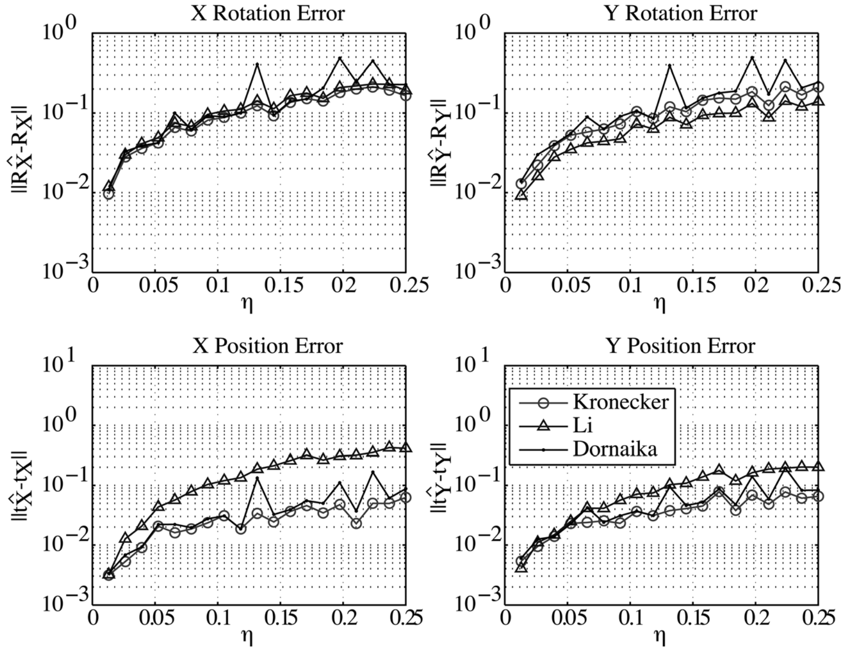

Fig. 2 Comparison of the Kronecker product method described in this paper (circles), the Li et al. Kronecker product method described in Ref. [9] (triangles), and the Dornaika and Horaud closed-form quaternion method described in Ref. [4] (solid line) on simulated data.

Kronecker method, which causes the larger positional errors that are illustrated in Fig. 2.

5.2 Real Data. In this section, the Kronecker method presented in this paper is compared with the Li et al. Kronecker method and results obtained from hand-calibration on real data obtained using a commercial system and a laser tracker system considered ground truth as shown in Fig. 3. The commercial system obtains rotational and positional data by matching features of a stationary object (O) in an image with features from a training image. These images are obtained from a camera (C) rigidly attached to a moving robot arm. Also attached to the robot arm is an active target (AT) that is being tracked by a stationary laser tracker (LT). Note that there is a rigid transformation $\mathbf{Y}$ between the camera and active target, since they are both rigidly attached to the robot arm. In addition, there is a rigid transformation $\mathbf{X}$ between the object and laser tracker, since they are both stationary. The robot arm is rotated about two of its rotational axes from ± 5 deg in increments of 5 deg. In addition, the robot arm is moved in the y direction from ± 150 mm in increments of 50 mm. Thus, the robot arm obtains $3 \times 3 \times 7 = 63$ positions. Data are obtained simultaneously for each system being time-stamped and synchronized at positions $j = 1, 2, \ldots, 63$. Mathematically, the relationship between the commercial system and the ground truth system can be described as

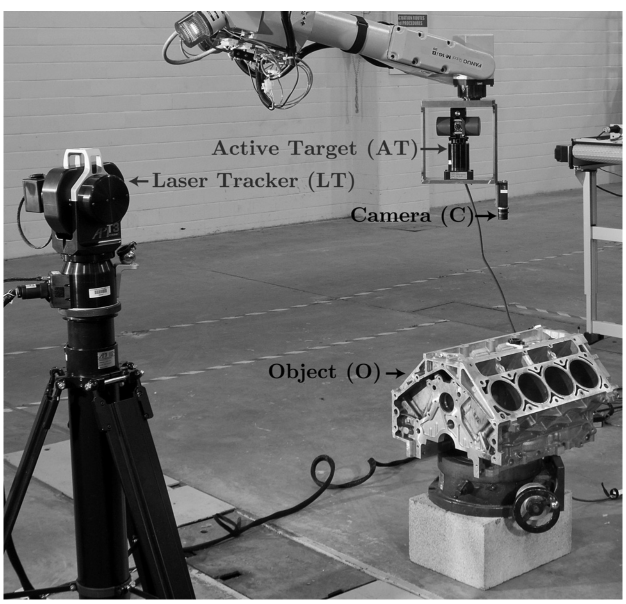

Fig. 3 Experimental setup of the commercial system with the laser tracker system

$$\underbrace{{}_{\mathrm{AT}}\mathbf{H}_{\mathrm{LT}}}_{\mathbf{A}_j} \cdot \underbrace{{}_{\mathrm{LT}}\mathbf{H}_{\mathrm{O}}}_{\mathbf{X}} = \underbrace{{}_{\mathrm{AT}}\mathbf{H}_{\mathrm{C}}}_{\mathbf{Y}} \cdot \underbrace{{}_{\mathrm{C}}\mathbf{H}_{\mathrm{O}}}_{\mathbf{B}_j}$$

Note that the commercial system also records if all of the features from the training image are detected in the image taken from the camera (C). For this experiment, 54 out of the 63 positions had all of the features presented in their corresponding images. Additional details of the experimental setup can be found in Ref. [26].

Experimental results for this setup are shown in Fig. 4 where the three graphs correspond to the error metrics outlined in Sec. 4. Specifically, calibration is performed using the 54 positions where all the features from the training image are detected. The $\mathbf{X}$ and $\mathbf{Y}$ obtained from this calibration are then used to determine the error in all 63 positions. Results obtained from the calibration using the Kronecker method presented in this paper are represented with circles, the Li et al. Kronecker method are described with triangles, and hand surveying the experimental setup with a laser tracker system, i.e., hand-calibration, are described with squares. The rotational errors for all three methods are nearly the same. However, the true discrepancies are shown in the translational errors. Notice that both Kronecker product methods produce better results than the hand-calibrated method which is prone to noise due to human error. The interesting difference is between the two Kronecker product translational errors. The errors exist since the positional results ($\mathbf{t}_X$ and $\mathbf{t}_Y$) for the Li et al. Kronecker method

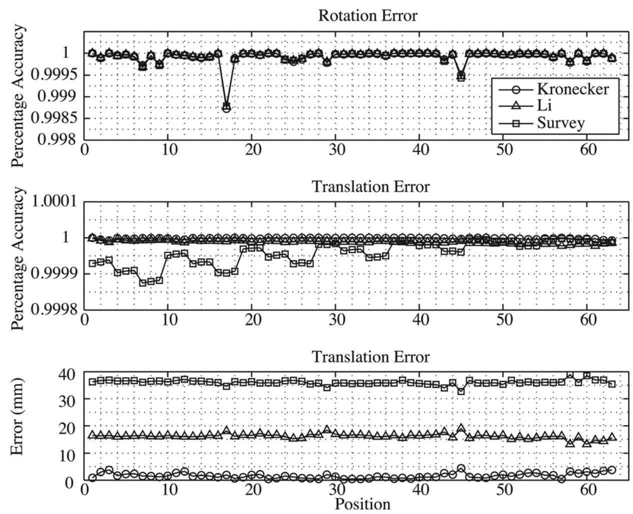

Fig. 4 Comparison of the Kronecker product method described in this paper (circles), the Li et al. Kronecker product method described in Ref. [9] (triangles), and hand-calibration results (squares) on real data.

were not re-calculated once the orientational results ($\mathbf{R_X}$ and $\mathbf{R_Y}$) were updated. Thus, errors are likely.

6 Conclusion

This paper constructs a closed-form solution for the robot-world/hand-eye calibration problem using the Kronecker product. This method is compared with the Kronecker product method by Li et al. and the closed-form quaternion method by Dornaika and Horaud on simulated data. In addition, the method is compared with the Kronecker product method by Li et al. and with hand-calibrated results on real data. It is shown that the Kronecker method that is presented in this paper is a reliable and accurate method for solving the robot-world/hand-eye calibration problem.

Acknowledgment

The author would like to thank Tsai Hong, Roger Eastman, and Tommy Chang for all their valuable discussions and suggestions on this paper. In addition, the author would like to acknowledge Robot Vision Technologies and the National Institute of Standards and Technology for providing test data sets. The author received an Intergovernmental Personnel Act (IPA) appointment from the National Institute of Standards and Technology (NIST). The problem discussed in this paper was formulated at NIST under the Measurement Science for Intelligent Manufacturing Robotics and Automation Program. Data were collected and analyzed within this program with results appearing in this paper.

References

[1] Shah, M., Eastman, R. D., and Hong, T., 2012, "An Overview of Robot-Sensor Calibration Methods for Evaluation of Perception Systems," Proceedings of the Workshop on Performance Metrics for Intelligent Systems, PerMIS'12, ACM, pp. 15–20.

[2] Strobl, K., and Hirzinger, G., 2006, "Optimal Hand-Eye Calibration," IEEE/RSJ International Conference on Intelligent Robots and Systems, pp. 4647–4653.

[3] Remy, S., Dhome, M., Lavest, J., and Daucher, N., 1997, "Hand-Eye Calibration," International Conference on Intelligent Robots and Systems, (IROS), Vol. 2, pp. 1057–1065.

[4] Dornaika, F., and Horaud, R., 1998, "Simultaneous Robot-World and Hand-Eye Calibration," IEEE Trans. Rob. Autom., **14**(4), pp. 617–622.

[5] Hirsh, R. L., DeSouza, G. N., and Kak, A. C., 2001, "An Iterative Approach to the Hand-Eye and Base-World Calibration Problem," International Conference on Robotics and Automation (ICRA), Vol. 3, pp. 2171–2176.

[6] Kim, S.-J., Jeong, M.-H., Lee, J.-J., Lee, J.-Y., Kim, K.-G., You, B.-J., and Oh, S.-R., 2010, "Robot Head-Eye Calibration Using the Minimum Variance Method," International Conference on Robotics and Biomimetics (ROBIO), IEEE, pp. 1446–1451.

[7] Yang, G., Chen, I.-M., Yeo, S. H., Lim, W. K., 2002, "Simultaneous Base and Tool Calibration for Self-Calibrated Parallel Robots," Robotica, **20**(4), pp. 367–374. Available at: http://155.69.254.10/users/risc/Pub/Conf/00-c-icarcv-simcal.pdf

[8] Zhuang, H., Roth, Z. S., and Sudhakar, R., 1994, "Simultaneous Robot/World and Tool/Flange Calibration by Solving Homogeneous Transformation Equations of the Form AX = YB," IEEE Trans. Rob. Autom., **10**(4), pp. 549–554.

[9] Li, A., Wang, L., and Wu, D., 2010, "Simultaneous Robot-World and Hand-Eye Calibration Using Dual-Quaternions and Kronecker Product," Inter. J. Phys. Sci., **5**(10), pp. 1530–1536.

[10] Ernst, F., Richter, L., Matthäus, L., Martens, V., Bruder, R., Schlaefer, A., and Schweikard, A., 2012, "Non-Orthogonal Tool/Flange and Robot/World Calibration," Int. J. Med. Rob. Comput. Assist. Surg., **8**(4), pp. 407–420.

[11] Shiu, Y. C., and Ahmad, S., 1989, "Calibration of Wrist-Mounted Robotic Sensors by Solving Homogeneous Transform Equations of the Form AX=XB," IEEE Trans. Rob. Autom., **5**(1), pp. 16–29.

[12] Tsai, R. Y., and Lenz, R. K., 1989, "A New Technique for Fully Autonomous and Efficient 3D Robotics Hand/Eye Calibration," IEEE Trans. Rob. Autom., **5**(3), pp. 345–358.

[13] Wang, C.-C., 1992, "Extrinsic Calibration of a Vision Sensor Mounted on a Robot," IEEE Trans. Rob. Autom., **8**, pp. 161–175.

[14] Park, F. C., and Martin, B. J., 1994, "Robot Sensor Calibration: Solving AX = XB on the Euclidean Group," IEEE Trans. Rob. Autom., **10**(5), pp. 717–721.

[15] Chou, J. C., and Kamel, M., 1991, "Finding the Position and Orientation of a Sensor on a Robot Manipulator Using Quaternions," Int. J. Robot. Res., **10**(3), pp. 240–254.

[16] Zhuang, H., Roth, Z., Shiu, Y., and Ahmad, S., 1991, "Comments on" Calibration of Wrist-Mounted Robotic Sensors by Solving Homogeneous Transform Equations of the Form AX = XB" [With Reply]," IEEE Trans. Rob. Autom., **7**(6), pp. 877–878.

[17] Horaud, R., and Dornaika, F., 1995, "Hand-Eye Calibration," Int. J. Robot. Res., **14**(3), pp. 195–210.

[18] Lu, Y.-C., and Chou, J. C., 1995, "Eight-Space Quaternion Approach for Robotic Hand-Eye Calibration," IEEE International Conference on Systems, Man and Cybernetics, **4**, pp. 3316–3321.

[19] Daniilidis, K., and Bayro-Corrochano, E., 1996, "The Dual Quaternion Approach to Hand-Eye Calibration," Proceedings of the 13th International Conference on Pattern Recognition, Vol. 1, pp. 318–322.

[20] Daniilidis, K., 1999, "Hand-Eye Calibration Using Dual Quaternions," Int. J. Robot. Res., **18**(3), pp. 286–298.

[21] Malti, A., and Barreto, J. P., 2010, "Robust Hand-Eye Calibration for Computer Aided Medical Endoscopy," International Conference on Robotics and Automation (ICRA), pp. 5543–5549.

[22] Chen, H. H., 1991, "A Screw Motion Approach to Uniqueness Analysis of Head-Eye Geometry," IEEE Proceedings of Computer Vision and Pattern Recognition (CVPR), pp. 145–151.

[23] Andreff, N., Horaud, R., and Espiau, B., 2001, "Robot Hand-Eye Calibration Using Structure From Motion," Int. J. Robot. Res., **20**(3), pp. 228–248.

[24] Laub, A. J., 2004, *Matrix Analysis for Scientists and Engineers*, Society for Industrial and Applied Mathematics, Philadelphia, PA.

[25] Shah, M., 2011, "Comparing Two Sets of Corresponding Six Degree of Freedom Data," Comput. Vis. Image Underst., **115**(10), pp. 1355–1362.

[26] Chang, T., Hong, T., Falco, J., Shneier, M., Shah, M., and Eastman, R., 2010, "Methodology for Evaluating Static Six-Degree-of-Freedom (6DOF) Perception Systems," Proceedings of the 10th Performance Metrics for Intelligent Systems Workshop, PerMIS'10, ACM, pp. 290–297.